Photosynth Res (2014) 119:15–29
DOI 10.1007/s11120-013-9818-1

REVIEW

The use and misuse of $V_{c,max}$ in Earth System Models

Alistair Rogers

Received: 18 November 2012 / Accepted: 19 March 2013 / Published online: 7 April 2013

Abstract Earth System Models (ESMs) aim to project global change. Central to this aim is the need to accurately model global carbon fluxes. Photosynthetic carbon dioxide assimilation by the terrestrial biosphere is the largest of these fluxes, and in many ESMs is represented by the Farquhar, von Caemmerer and Berry (FvCB) model of photosynthesis. The maximum rate of carboxylation by the enzyme Rubisco, commonly termed $V_{c,max}$, is a key parameter in the FvCB model. This study investigated the derivation of the values of $V_{c,max}$ used to represent different plant functional types (PFTs) in ESMs. Four methods for estimating $V_{c,max}$ were identified; (1) an empirical or (2) mechanistic relationship was used to relate $V_{c,max}$ to leaf N content, (3) $V_{c,max}$ was estimated using an approach based on the optimization of photosynthesis and respiration or (4) calibration of a user-defined $V_{c,max}$ to obtain a target model output. Despite representing the same PFTs, the land model components of ESMs were parameterized with a wide range of values for $V_{c,max}$ (−46 to +77 % of the PFT mean). In many cases, parameterization was based on limited data sets and poorly defined coefficients that were used to adjust model parameters and set PFT-specific values for $V_{c,max}$. Examination of the models that linked leaf N mechanistically to $V_{c,max}$ identified potential changes to fixed parameters that collectively would decrease $V_{c,max}$ by 31 % in C_3 plants and 11 % in C_4 plants. Plant trait data bases are now available that offer an excellent opportunity for models to update PFT-specific parameters used to estimate $V_{c,max}$. However, data for parameterizing some PFTs, particularly those in the Tropics and the Arctic are either highly variable or largely absent.

Keywords Rubisco · $V_{c,max}$ · Leaf nitrogen · Earth System Models

A. Rogers (✉)
Department of Environmental Sciences, Brookhaven National Laboratory, Upton, NY 11973, USA
e-mail: arogers@bnl.gov

Introduction

The primary goal of Earth System Models (ESMs) is to improve understanding and projection of future global change. Since global change is driven principally by the increase in atmospheric CO_2 concentration ($[CO_2]$), projection of future $[CO_2]$ is a primary product of the models. Therefore, uncertainty in the estimation of the large CO_2 fluxes associated with the global C cycle will have a marked impact on projected global change. Photosynthetic CO_2 uptake by the terrestrial biosphere is the largest of these fluxes and the entry point of C into the terrestrial C sink that currently subsidizes anthropogenic fossil fuel use. It is therefore critical that ESMs accurately model photosynthesis (Canadell et al. 2007; Beer et al. 2010). However, current understanding and model representation of the terrestrial C cycle, and the response of the terrestrial C cycle to rising $[CO_2]$ and temperature, are among the greatest uncertainties in ESMs in terms of both scientific understanding and model representation (Knorr 2000; Friedlingstein et al. 2006; Gregory et al. 2009; Smith and Dukes 2012).

Photosynthetic CO_2 uptake is well-described by the Farquhar, von Caemmerer and Berry (FvCB) model of photosynthesis (Farquhar et al. 1980) and many ESMs use a derivation of this model to estimate gross primary production (GPP). One of the key parameters required by the FvCB model is an estimate of the maximum rate of

carboxylation by the enzyme Rubisco (EC number 4.1.1.39), commonly termed $V_{c,max}$. Sensitivity analysis of ESMs has shown that projections of net primary production (NPP) are particularly sensitive to fixed parameters associated with estimating $V_{c,max}$ from leaf N content (Friend 2010) and model uncertainty over the parameter $V_{c,max}$, has been shown to account for a c. 30 Pg C year^{-1} variation in model estimation of GPP (Bonan et al. 2011). Given that anthropogenic CO_2 sources add c. 9 Pg C year^{-1} to the atmosphere (Boden et al. 2012), the uncertainty associated with estimation of $V_{c,max}$, and the need to constrain this estimate are obvious. In many models $V_{c,max}$ is not only the key parameter for estimating photosynthesis, but also, through a simple multiplier, autotrophic respiration (Knorr 2000; Kucharik et al. 2000; Sitch et al. 2003; Biome-BGC 2010). In other words, accurate representation of $V_{c,max}$ is critical not only just for modeling global GPP but also for NPP. Simply stated, $V_{c,max}$ is one of the most critical parameters for the successful projection of future global change. The aim of this study was to examine the different ways in which $V_{c,max}$ is derived for use in ESMs, examine some of the key assumptions, and suggest some opportunities for improving the representation of $V_{c,max}$ in these models.

Models investigated

The key land model components of ESMs were identified from the fourth and fifth phases of the Coupled Climate Carbon Cycle Model Intercomparison Project, commonly known as CMIP4 (Friedlingstein et al. 2006) and CMIP5 (Arora et al. 2013), and from a recent review on respiration and photosynthesis in global scale models (Smith and Dukes 2012). Since the focus of this study was to examine the use of $V_{c,max}$ in ESMs, the scope was restricted to models where $V_{c,max}$ was used to simulate photosynthesis using the FvCB model. As a result several models that use alternative approaches, such as CASA, GTEC, SEIB-DGVM, SLAVE, Sheffield-DGVM, TEM, and VEGAS were not considered (McGuire et al. 1992; Potter et al. 1993; Friedlingstein et al. 1995; King et al. 1997; Woodward and Lomas 2004; Zeng et al. 2004; Sato et al. 2007).

All the models investigated used plant functional types (PFTs) to describe the landscape. Grouping species into PFTs allows the complexity of diverse communities to be reduced to a few key PFTs. Each PFTs can then be parameterized with relevant traits. When coupled with estimation of community composition this allows models to link plant physiology and ecosystem processes, and when sufficient PFTs are used, provides a higher resolution than classifying vegetation by biomes alone. In most models, gas exchange and energy balance calculations happen separately for each PFT, as a result the number of calculations, and required computer power, scales linearly with PFT number. With a finite resource, increasing the resolution of a model by adding PFTs is tradeoff between other kinds of resolution e.g., time steps, vertical resolution, and the accuracy of iteratively solved processes. Typically the models include many plant traits in their PFT definitions and that information covers a range of ecosystem processes, of which $V_{c,max}$ is one. The number of PFTs used by the models varied from 5 to 16 with the richer models dividing broad PFT definitions into additional categories.

Eleven models were investigated, and four main approaches for estimating $V_{c,max}$ emerged; (1) an empirical relationship between $V_{c,max}$ and leaf N content, (2) a mechanistic relationship between $V_{c,max}$ and leaf N content, (3) an estimation based on the theory that a leaf will optimize the tradeoff between photosynthesis and respiration (Haxeltine and Prentice 1996b), and (4) calibration of fixed $V_{c,max}$ values to obtain a target model output.

Unless specified, all discussion of $V_{c,max}$ assumes normalization to 25 °C. Temperature corrections associated with CO_2 assimilation in ESMs has been covered recently and is not discussed here (Smith and Dukes 2012). The $V_{c,max}$ values presented here refer to upper canopy sunlit foliage. Detailed comparison of the different approaches used to attenuate $V_{c,max}$ with canopy depth is beyond the scope of this study, but typically $V_{c,max}$ is decreased with canopy depth through a gradient in leaf N content that is specified through leaf area index, specific leaf area, or by the use of a nitrogen profile coefficient (Friend and Kiang 2005; Biome-BGC 2010; Oleson et al. 2010; Zaehle and Friend 2010; Clark et al. 2011; Bonan et al. 2012).

Empirical relationship

BETHY & JSBACH

The Biosphere Energy Transfer Hydrology Scheme (Knorr 2000; Ziehn et al. 2011) estimates $V_{c,max}$ (μmol m^{-2} leaf area s^{-1}) from the linear relationship with leaf N content (Kattge et al. 2009).

$$V_{c,max} = i_v + s_v \times N_a \quad (1)$$

where the intercept (i_v) and slope (s_v) for $V_{c,max}$ as a function of leaf N content expressed on an area basis (N_a, g m^{-2} leaf area) are derived for each PFT. BETHY uses an extensive data base of $V_{c,max}$ values (723 data points), and $V_{c,max}$ values determined by standardized model inversions of the maximum photosynthetic rate (A_{max}, 776 data points) to determine the PFT-specific values for i_v and s_v. Then, a larger data base of N_a is used to provide additional data (1966 total data points) for the determination of PFT-specific $V_{c,max}$ values (Kattge et al. 2009). Representation

of photosynthesis and estimation of $V_{c,max}$ in 13 PFTs within the Joint Scheme for Biosphere Atmosphere Coupling in Hamburg (JSBACH) is based on BETHY (Raddatz et al. 2007).

Hybrid and HyLand

Hybrid 6.5 (Friend 2010) obtains $V_{c,max}$ by multiplying N_a by a proportionality coefficient n_2 (Kull and Kruijt 1998). The coefficient n_2 (0.23 μmol CO_2 mmol N^{-1} s^{-1}) was derived from 45 measurements of $V_{c,max}$ and leaf N made on two tree (*Populus tremula*, *Corylus avellana*) and one shrub (*Tilia cordata*) species (Kull and Niinemets 1998). To account for variation in n_2 between PFTs an additional cooefficient, n_f (photosynthetic N factor or relative photosynthetic capacity parameter) is used to adjust n_2 by −10 to +50 % (Friend and Kiang 2005; Friend 2010).

$$V_{c,max} = N_a \times n_2 \times n_f \times \frac{1000}{M_N} \quad (2)$$

where M_N = molecular mass of N (14 g mol^{-1}). Calibration against eddy flux data from mixed rain forest, evergreen forest, deciduous forest, and wheat (Wofsy et al. 1993; Goulden et al. 1996; Malhi et al. 1998; Berbigier et al. 2001; Hanan et al. 2002) provided values for n_f for some PFTs, but others were estimated based on similarity to the PFTs that were dominant in the flux data calibration. For example, the n_f for Arctic tundra is estimated as $0.75n_f$ deciduous forest $+0.25n_f$ rain forest (Friend and Kiang 2005). HyLand is a simplified version of the Hybrid model where the representation of photosynthesis, and the derivation of $V_{c,max}$ are unaltered (Levy et al. 2004).

O–CN

The O–CN model (Zaehle and Friend 2010) is an extension of ORCHIDEE (described below) that includes key N cycle processes. Unlike ORCHIDEE, O–CN contains an explicit link between $V_{c,max}$ and leaf N content. In O–CN, $V_{c,max}$ is estimated using the canopy photosynthesis and conductance model employed by Hybrid (Friend and Kiang 2005), where the leaf N content for a given canopy layer is used to estimate the $V_{c,max}$ in that layer,

$$V_{c,max} = n_{fO-CN} \frac{f_{Np}}{f_{Np,ave}} \times \frac{N_a \times 1000}{M_N} \quad (3)$$

where n_{fO-CN} (μmol CO_2 mmol $N^{-1}s^{-1}$) is a PFT-specific parameter linking N_a to photosynthetic potential at an average observed leaf N content ($N_{a,ave}$) for a specific PFT. Based on the linear relationship describing the amount of N invested in non-photosynthetic processes (Friend et al. 1997) the fraction of leaf N in the photosynthetic apparatus (f_{Np}, which includes N partitioned to apparatus associated with both the light and dark reactions of photosynthesis) for a given N_a is,

$$f_{Np} = a_{Np} + b_{Np} \times N_a \quad (4)$$

where a_{Np} is the minimum fraction of leaf N associated with photosynthesis, a_{Np} *is* set at 0.33 and 0.17 for broad leaf and needle leaf PFTs, respectively (Evans 1989). The slope of the relationship between N_a and f_{Np} (b_{Np}) is set at 0.0714 (Evans 1989; Zaehle and Friend 2010). The $f_{Np,ave}$ is the f_{Np} for a given PFT where $N_a = N_{a,ave}$ (Zaehle and Friend 2010). The $N_{a,ave}$ is calculated from PFT-specific values of *SLA* (m^2 leaf area C g^{-1}), and average leaf N content expressed on a dry mass basis (N_m, %), assuming a C content (C_m) of 48 % dry mass (Reich et al. 1997; White et al. 2000; Zaehle and Friend 2010).

$$N_{a,ave} = \frac{\frac{N_{m,ave}}{c_m}}{SLA} \quad (5)$$

O–CN constrains possible N_a by imposing limitations on the minimum and maximum N_m values possible for each PFT. The data set used to parameterize the 12 PFTs for $N_{m,ave}$ (White et al. 2000) is the same source that was used to parameterize CLM and Biome-BGC (see below). The data listed by White et al. (2000) cover a wide range of species with over 150 data entries but there are some important gaps and under-represented PFTs e.g., C_4 grasses and shrubs.

JULES

The Joint UK Land Environment Stimulator (JULES) model (version 2.2) is coupled to the MOSES 2 land-surface scheme and the TRIFFID dynamic global vegetation model. JULES estimates $V_{c,max}$ from leaf N content for five PFTs (Schulze et al. 1994; Cox 2001; Clark et al. 2011). $V_{c,max}$ is assumed to be linearly related to leaf nitrogen concentration.

$$V_{c,max} = n_e \times n_l \quad (6)$$

where n_l is the leaf N content (kg N kg C^{-1}) and n_e is a constant relating leaf N to Rubisco carboxylation capacity that is 0.0008 and 0.0004 mol CO_2 m^{-2} s^{-1} kg C kgN^{-1} for C_3 and C_4 plants, respectively (Cox 2001; Clark et al. 2011). The values for n_e were derived from assumptions and regressions in Schulze et al. (1994) and are elucidated below,

$$n_e = C_m \times S_{R1} \times S_{R2} \times S_{R3} \times S_{A2} \times 0.001 \quad (7)$$

where the fraction of leaf dry matter in the form of C (C_m) is 0.4. The regression slopes S_{R1}, S_{R2}, and S_{R3}, (0.3012, 2.996, and 1.048, respectively) empirically link observations of leaf N concentration to maximum stomatal conductance, maximal stomatal conductance to maximum

surface conductance, and maximimum surface conductance to maximum surface assimilation rate (Fig. 3 in Schulze et al. 1994). The data sets used to generate the regressions described above are extensive and were compiled from over 50 studies and included data from over 200 species covering all major biomes. The theory behind the link between leaf, canopy, and ecosystem fluxes is described in detail by Schulze et al. (1994). The final assumption, S_{A2}, is that the maximum surface assimilation rate is 0.5 $V_{c,max}$ for C_3 plants and equal to $V_{c,max}$ for C_4 plants.

In the Hadley Centre technical note that describes TRIFFID (Cox 2001), the values for n_l are derived from Schulze et al. (1994) as described above. In the more recent description of JULES (Clark et al. 2011), the values for n_l from Schulze et al. (1994) have been updated. This was the result of a model calibration exercise where JULES was coupled to the atmospheric model as part of HadGEM2-ES (the Earth System version of the Met Office Hadley Centre HadGEM2 model) and various parameter values were changed to match observed vegetation distribution, carbon stores, and fluxes (Clark, personnel communication). The resulting updated values for $V_{c,max}$ in JULES are smaller for 4 of the 5 PFTs when compared to the values in the previous model description (Cox 2001) this is most marked for the shrub PFT, where $V_{c,max}$ is 50 % smaller.

Mechanistic relationship

Biome-BGC and the Community Land Model

Biome-BGC version 4.2 and the Community Land Model (CLM) version 4.0 (Biome-BGC 2010; Oleson et al. 2010) estimate $V_{c,max}$ using a more mechanistic approach that is constrained by constants associated with the structure, function, and amount of Rubisco in the leaf. CLM estimates $V_{c,max}$ from PFT-specific parameters of N_a and the fraction of that N invested in Rubisco (F_{LNR}, g N in Rubisco g^{-1} N). F_{NR} is the mass ratio of total Rubisco molecular mass to N in Rubisco (g Rubisco g^{-1} N in Rubisco). The specific activity of Rubisco at 25 °C (α_{R25}, μmol CO_2 g^{-1} Rubisco s^{-1}) is set at 60 μmol CO_2 g^{-1} Rubisco s^{-1} (Woodrow and Berry 1988). Recently, canopy processes in CLM were updated but the derivation of $V_{c,max}$ as described by Eq. 8 and the values for the fixed parameters in that equation are unaltered in the revised model (Bonan et al. 2011, 2012).

$$V_{c,max} = N_a \times F_{LNR} \times F_{NR} \times \alpha_{R25} \quad (8)$$

The value for N_a is derived from PFT-specific variables for the leaf C:N ratio (CN_L, gC g^{-1}N) and the SLA.

$$N_a = \frac{1}{CN_L \times \mathrm{SLA}} \quad (9)$$

The parameters used for the different PFTs in CLM are provided in a technical note (Oleson et al. 2010) and derived from the parameterization used in Biome-BGC (White et al. 2000). Due to insufficient data from which to parameterize F_{LNR}, White et al. (2000) calculated F_{LNR} from a review of $V_{c,max}$ values in 109 species (Wullschleger 1993), and their own data sets for SLA and CN_L following Eq. 8. Shrub F_{LNR} was based on hot shrubs only and set to the value for evergreen needle leaf forest. The F_{LNR} for deciduous needle leaf forest was set to match that used for deciduous broad leaf forest, and the F_{LNR} for evergreen needle leaf forests was increased by one standard deviation because the measurement temperatures were generally lower than for other biomes (PFT nomenclature follows White et al. 2000).

Biome-BGC (v4.2) calculates $V_{c,max}$ using a mathematically identical method to CLM (Thornton et al. 2002; Biome-BGC 2010). BIOME-BGC is typically run with six PFTs (Wang et al. 2011) parameterized as described by White et al. (2000).

$$V_{c,max} = N_a \times F_{LNR} \times 7.16 \times \mathrm{ACT} \quad (10)$$

where 7.16 is the mass ratio of total Rubisco molecular mass to N in Rubisco (equivalent to F_{NR} in CLM) and ACT is the specific activity of Rubisco, equivalent to α_{R25} in CLM and also derived from the same kinetic constants (Woodrow and Berry 1988). Leaf N_a content is a function of the user-defined ratio of C:N and SLA as described above for CLM (Eq. 9).

The CLM includes a full prognostic N cycle, referred to as CLM–CN which introduces a down regulation of canopy photosynthesis based on the availability of mineral N to support new growth which impacts $V_{c,max}$ through changes in CN_L. A prescribed PFT-specific N availability factor, $f(N)$, was derived so that simulated photosynthetic rate was comparable to the realized rate when the CN module was active. This allows CLM to run with the biogeochemistry module (CN) turned off, but still represent the impact of N availability on photosynthesis (Oleson et al. 2010). Adjustment of standard CLM $V_{c,max}$ values with $f(N)$ decreases $V_{c,max}$ by 17–40 %.

$$V_{c,max-CN} = V_{c,max} \times f(N) \quad (11)$$

Optimization of resources

LPJ

The Lund-Potsdam-Jena model (Sitch et al. 2003) calculates GPP for 10 PFTs following the approach used in BIOME3 (a predecessor to Biome-BGC that uses a different approach to estimate $V_{c,max}$), where GPP is calculated as a function of absorbed photosynthetically active radiation (APAR) based on an alternative version of the FvCB model (Haxeltine and Prentice 1996a). A fixed

$V_{c,max}$ is not prescribed for each PFT but is calculated using an optimization algorithm which is described in detail elsewhere (Haxeltine and Prentice 1996b). Succinctly, $V_{c,max}$ is calculated to obtain the highest net CO_2 uptake based on tradeoff between the advantage of having a high Rubisco activity versus the respiratory cost of maintaining it. A high net photosynthetic rate at a high APAR can be achieved by having a high $V_{c,max}$, but the respiratory cost is relatively high at low APAR and low CO_2 uptake. Thus for any APAR there is an optimal investment in Rubisco that produces the highest net photosynthetic rate. The algorithm also accounts for photoperiod, and leaf age in conifers (Haxeltine and Prentice 1996a, b; Sitch et al. 2003). LPJ also includes a global dynamic *N* model with full interaction with *C*, *N* and water cycles (Xu and Prentice 2008).

IBIS

The Integrated Biosphere Simulator (IBIS) version 2 (Foley et al. 1996; Kucharik et al. 2000) proscribes constant values of $V_{c,max}$ at 15 °C for 12–15 PFTs. In the original IBIS, $V_{c,max}$ was estimated by predicting the maximum $V_{c,max}$ (without water stress or *N* limitation) possible that maintains an optimal balance between gross and maintenance respiration as described above for LPJ (Haxeltine and Prentice 1996b). This dynamic prediction of $V_{c,max}$ was dropped from IBIS-2 for the sake of simplicity. The values used in IBIS-2 are for upper canopy sun lit foliage. The source of these values is unclear. Because IBIS-2 did not use the optimization procedure implemented in IBIS (Haxeltine and Prentice 1996b) a new approach was adopted where the photosynthetic rate of upper canopy foliage was scaled in proportion to the APAR within it (Kucharik et al. 2000). In this study, the values of $V_{c,max}$ at 15 °C were adjusted to 25 °C for model comparison (Bernacchi et al. 2001).

ORCHIDEE

The Organizing Carbon and Hydrology in Dynamic Ecosystems model (Krinner et al. 2005) represents photosynthesis in a sub model, STOMATE (Saclay Toulouse Orsay Model for the Analysis of Terrestrial Ecosystems). ORCHIDEE has 12 PFTs which are parameterized following LPJ (Sitch et al. 2003), but the approach for parameterizing $V_{c,max}$ is different. Each PFT has a prescribed optimum photosynthesis temperature (T_{opt}) and a corresponding $V_{c,max}$opt (unstressed, $V_{c,max}$ measured at optimum temperature). The T_{opt} for C_3 grasses and C_3 crops is calculated as a function of multiannual mean temperature for C_3 grasses to account for the presence of these PFTs in a large range of ecosystems. $V_{c,max}$opt is adjusted to account for changes in carboxylation capacity with leaf age and canopy position, neither adjustment is explicitly linked to leaf *N* content (Johnson and Thornley 1984; Ishida et al. 1999). The source of the values for $V_{c,max}$opt is unclear. In this study values for $V_{c,max}$opt were adjusted to 25 °C to facilitate comparison with other models (Bernacchi et al. 2001).

Model calibration

AVIM

The Atmosphere-Vegetation Interaction Model (AVIM) is the land carbon cycle component of the Beijing Climate Center model. The AVIM model calculates a temperature corrected $V_{c,max}$, as a function of nitrogen concentration and soil moisture (Lu and Ji 2006).

$$V_{c,max-N_{ws}} = V_{c,max} \times f(N) \times f(w_s) \quad (12)$$

Calculation of $V_{c,max}$ in AVIM is based on CLM3, where $V_{c,max\text{-}Nws}$ is the value of $V_{c,max}$ following correction for *N* and water availability. Both $f(N)$ and $f(w_s)$ are heuristic functions ranging from 0 to 1, where 1 is no limitation on $V_{c,max}$ due to nitrogen limitation or soil moisture availability, respectively (Ji 1995; Bonan 1996; Sellers et al. 1996; Lu and Ji 2006). In CLM3, $V_{c,max}$ values were obtained from published estimates (Wullschleger 1993; Kucharik et al. 2000; Oleson et al. 2004). Currently $V_{c,max\text{-}Nws}$ is not corrected for *N* availability, i.e., $f(N) = 1$, because estimates of $V_{c,max}$ already account for potential *N* limitation (Bonan 1996). The function adjusting $V_{c,max}$ for water availability, $f(w_s)$, is also set to 1, i.e., no limitation (Bonan 1996). Therefore both $f(N)$ and $f(w_s)$ are essentially unused, and parameterization of AVIM is purely through a user-defined parameter. Although AVIM uses the same PFT definitions as CLM3 (Oleson et al. 2004) the values for $V_{c,max}$ were calibrated with remotely sensed estimates of GPP and through the Ecosystem Model-Data Intercomparison project, estimates of NPP (Ji, personal communication). This calibration adjusted CLM3 $V_{c,max}$ values by −15 to +353 %.

CTEM

The photosynthesis sub-module used in the Canadian Terrestrial Ecosystem Model (CTEM 1.0) is implemented as in the Simple Biosphere Model 2 (SiB2), where $V_{c,max}$ is an input parameter that is varied for different model applications (Sellers et al. 1996; Arora 2003; Arora and Boer 2010). When used in the Canadian Center for Climate Modeling and Analysis Earth System Model, CTEM is parameterized with nine PFTs. For CTEM 1.0 values for $V_{c,max}$ were derived from unspecified sources and then tuned to reproduce observed global spatial patterns in GPP.

An updated parameterization (CTEM 1.1, Arora, personal communication) is based on published PFT-specific values of $V_{c,max}$ (Scholze et al. 2007; Kattge et al. 2009) which are subsequently calibrated to match site level or global estimates of productivity and NPP/GPP ratios (Luyssaert et al. 2007; Zhang et al. 2009; Beer et al. 2010). In most cases, calibration occurs within the standard deviations of the estimates for $V_{c,max}$ listed by Kattge et al. (2009).

Representation of $V_{c,max}$ by PFTs

Due to lack of clarity in model descriptions or the approach taken to model $V_{c,max}$, PFT-specific values for $V_{c,max}$ were not readily available for all models, so where possible this information was obtained directly from the modeling groups. Ten PFT data sets were identified for $V_{c,max}$ (Table 1). Of these, a range (5–16) of PFTs was used to represent the terrestrial biosphere. However, in several models the same $V_{c,max}$ is used to represent a number of PFTs so the range of $V_{c,max}$ values is typically smaller. Figure 1 shows the range of $V_{c,max}$ values from the models in Table 1 conflated into 16 common PFT definitions. There is considerable variation between the values of $V_{c,max}$ used to represent a given PFT. Across all PFTs the average range of $V_{c,max}$ values was −46 to +77 % of the PFT mean. The range of $V_{c,max}$ values used to parameterize evergreen and deciduous trees in the tropics was particularly large, and only 4 models included a PFT for Arctic vegetation.

Model parameters and assumptions

The models outlined above have both PFT-specific parameters and fixed parameters, in the algorithms used to estimate $V_{c,max}$. Some also include PFT-specific coefficients that are used to adjust fixed parameters. The aim of the next section is to examine the assumptions underlying the values that are used for fixed parameters, and where possible, offer suggestions for improvements.

Leaf traits

Many of the models include leaf traits in their estimation of $V_{c,max}$. These traits have traditionally been obtained from the literature or from private data bases. The TRY database now offers a central portal through which to access global plant trait data from many sources (Kattge et al. 2011). As awareness, confidence and data submission to TRY grows it is hoped that ESMs can use the large amount of trait data to constrain input parameters, or at least agree to use the same numbers. Improved parameterization of a leaf level model using trait databases has been shown to constrain estimates of photosynthesis, which suggests that this approach could also be used effectively to parameterize ESMs (Ziehn et al. 2011). In addition, well-established correlations among leaf traits, that include SLA, and N_a, can be used to markedly reduce model uncertainty when multitrait covariance is incorporated into the models (Wang et al. 2012).

Currently different sources of trait data are used, resulting in variation among model input. For example, leaf C content (C_m, %) is a fixed parameter in some models but varies from 40 to 50 % (JULES, O–CN, Biome-BGC). The variation in N_a is also substantial. The six models reporting sufficient information to calculate N_a for two commonly defined PFTs show that for temperate broadleaf deciduous trees the PFT defined N_a ranged from 1.03 to 1.73 g m^{-2} and in C_3 grasses ranged from 0.82 to 1.74 g m^{-2} (BETHY, Biome-BGC, CLM, Hybrid, JULES, O–CN).

Metadata associated with traits will be important for accurate scaling and modeling. For example N_a may be derived from an entire leaf, a lamina, or a lamina section. When linking N_a to a photosynthetic parameter the most appropriate measurement of N_a will come from the section of leaf enclosed by the gas exchange cuvette, which may not include large veins. Scaling this relationship to the leaf in the most accurate way would require estimates of N_a based on the entire lamina, whereas modeling construction costs of foliage would require the petiole to be included in the estimate. The parameter $V_{c,max}$ is subject to even more confounding variables, these include: photoperiod length, time of day, day of year, the measurement protocol, subsequent modeling approaches, and temperature corrections (Bernacchi et al. 2001; Wilson et al. 2000; Long and Bernacchi 2003; Xu and Baldocchi 2003; Ethier and Livingston 2004; Gu et al. 2010; Bauerle et al. 2012; Smith and Dukes 2012). This poses a real challenge to databases. A possible solution to the problem of post measurement variation in modeling $V_{c,max}$ was recently offered (Gu et al. 2010). They established a service-in-exchange-for-data-sharing website where they provide analysis of leaf gas exchange measurements and in return the gas exchange data used to compute $V_{c,max}$ are stored and made freely available to the community. In time this project may offer the chance to re-compute large data sets using common protocols.

The fraction of leaf N invested in Rubisco (F_{LNR})

Of central importance to modeling photosynthesis and linking that estimation to the N cycle is the link between $V_{c,max}$ and leaf N content. In CLM and Biome-BGC, the PFT-specific parameter F_{LNR} (Eq. 8 and 10) sets potential rates of carboxylation as a function of leaf N content, and is a dominant control on photosynthesis. A recent sensitivity analysis of 80 CLM input parameters identified the

Table 1 Values of $V_{c,max}$ at 25 °C for the plant functional types (PFTs) listed in the models investigated

Model	Plant functional type	$V_{c,max}$ (μmol m^{-2} s^{-1})
AVIM	Needle leaf evergreen temperate tree	60
	Needle leaf evergreen boreal tree	58
	Needle leaf deciduous boreal tree	68
	Broad leaf evergreen tropical tree	64
	Broad leaf evergreen temperate tree	68
	Broad leaf deciduous tropical tree	56
	Broad leaf deciduous temperate tree	60
	Broad leaf deciduous boreal tree	65
	Broad leaf evergreen shrub	60
	Broad leaf deciduous temperate shrub	52
	Broad leaf deciduous boreal shrub	56
	C_3 arctic grass	55
	C_3 non-arctic grass	40
	C_4 grass	25
	Crop	55
BETHY	Tropical tree (oxisols)	28
	Tropical tree (non-oxisols)	36
	Temperate broad leaf evergreen tree	58
	Temperate broad leaf deciduous trees	54
	Evergreen coniferous forest	58
	Deciduous coniferous trees	36
	Evergreen shrubs	65
	Deciduous shrubs	65
	C_3 grass	71
	C_4 grass	20
	Tundra vegetation	20
	Crops	90
Biome-BGC	Evergreen needle leaf forest	34
	Evergreen broad leaf forest	51
	Deciduous broad leaf forest	47
	C_3 grass	60
	C_4 grass	60
	Shrub	34
CLM	Needle leaf evergreen tree—temperate	44 (61)
	Needle leaf evergreen tree—boreal	42 (54)
	Needle leaf deciduous tree—boreal	45 (57)
	Broad leaf evergreen tree—tropical	59 (72)
	Broad leaf evergreen tree—temperate	51 (72)
	Broad leaf deciduous tree—tropical	34 (52)
	Broad leaf deciduous tree—temperate	33 (52)
	Broad leaf deciduous tree—boreal	36 (52)
	Broad leaf evergreen shrub—temperate	44 (72)
	Broad leaf deciduous shrub—temperate	31 (52)
	Broad leaf deciduous shrub—boreal	39 (52)
	C_3 Arctic grass	35 (52)
	C_3 grass	31 (52)
	C_4 grass	33 (52)
	Crop 1	35 (57)
	Crop 2	35 (57)

Table 1 continued

Model	Plant functional type	$V_{c,max}$ (μmol m^{-2} s^{-1})
CTEM	Needle leaf evergreen	50 (35)
	Needle leaf deciduous	70 (40)
	Broad leaf evergreen	35 (51)
	Broad leaf deciduous—cold	65 (67)
	Broad leaf deciduous—dry	65 (40)
	C_3 crop	80 (100)
	C_4 crop	40 (40)
	C_3 grass	70 (75)
	C_4 grass	30 (15)
Hybrid	Tundra	37
	Grassland	20
	Shrub	51
	Woodland	22
	Deciduous	31
	Evergreen	43
	Rain forest	49
	Crops	53
IBIS	Tropical broad leaf evergreen	163
	Tropical broad leaf drought-deciduous	163
	Temperate broad leaf evergreen	100
	Temperate conifer evergreen	75
	Temperate broad leaf cold deciduous	75
	Boreal conifer evergreen	63
	Boreal broad leaf cold-deciduous	75
	Boreal conifer cold deciduous	75
	Evergreen shrub	69
	Cold-deciduous shrub	69
	Cool grass	63
	Warm grass	38
JULES	Broad leaf tree	37
	Needle leaf tree	26
	C_3 grass	58
	C_4 grass	24
	Shrub	48
O–CN	Tropical broad leaved evergreen	24
	Tropical broad leaved rain green	20
	Temperate needle leaved evergreen	17
	Temperate broad leaved evergreen	59
	Temperate broad leaved summer green	20
	Boreal needle leaved evergreen	17
	Boreal broad leaved summer green	20
	Boreal needle leafed summer green	27
	C_3 herbaceous	20
	C_4 herbaceous	13
	C_3 crop	20
	C_4 crop	13
ORCHIDEE	Tropical broad leaf evergreen trees	18
	Tropical broad leaf rain green trees	22

Table 1 continued

Model	Plant functional type	$V_{c,max}$ (μmol m^{-2} s^{-1})
	Temperate needle leaf evergreen trees	32
	Temperate broad leaf evergreen trees	21
	Temperate broad leaf summer green trees	29
	Boreal needle leaf evergreen trees	38
	Boreal broad leaf summer green trees	38
	Boreal needle leaf summer green trees	28
	Natural C_3 grass	56
	Natural C_4 grass	28
	Agricultural C_3 grass	73
	Agricultural C_4 grass	28

Values were derived from the equations and data listed in the model descriptions with the exception of AVIM (personal communication, Ji), Biome-BGC (personal communication, Running), and CTEM 1.1 (personal communication, Arora). The values for ORCHIDEE and IBIS were adjusted from published values to 25 °C to allow comparison with other models (Bernacchi et al. 2001). CLM is usually run either with the biogeochemistry module turned on or with $V_{c,max}$ adjusted to account for N availability (Eq. 11). Therefore CLM–CN values are listed, for reference the unadjusted CLM values are shown in parentheses. The CTEM 1.1 values have not yet been used widely and therefore CTEM 1.0 values are listed with the updated CTEM 1.1 values shown in parentheses

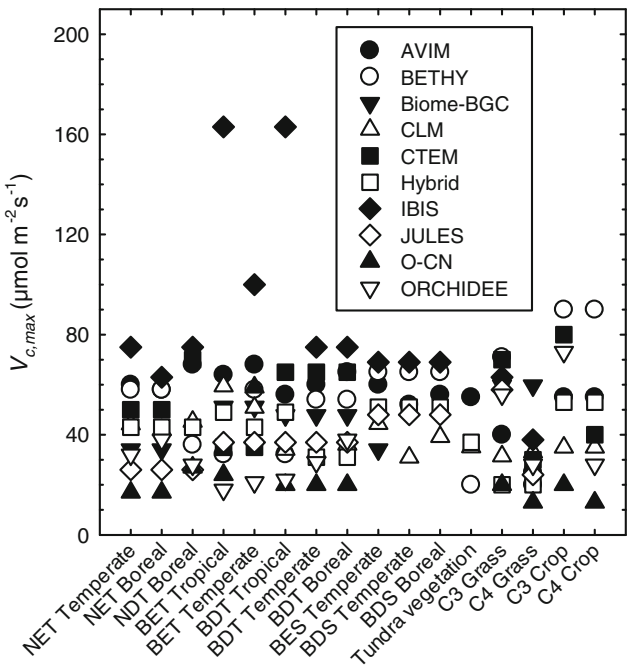

Fig. 1 The maximum rate of carboxylation by Rubisco ($V_{c,max}$) for 16 plant functional types (PFTs) derived from the models described in Table 1. For a given PFT a value for $V_{c,max}$ was assigned from each model based on the similarity to the original PFT description. Where a PFT is delineated to a greater extent than in the original model the most appropriate $V_{c,max}$ value is repeated for that PFT division. Where no $V_{c,max}$ value was assigned to a PFT, no data were included from that model. BETHY classified tropical trees based on soil type (Table 1). The mean $V_{c,max}$ for oxisols and non-oxisols from BETHY was used to represent both tropical PFTs in this figure. Values for CLM were for CLM–CN and values for CTEM were for CTEM 1.0. PFT abbreviations; *N* needle leaf, *B* broad leaf, *E* evergreen, *D* deciduous, *T* tree, *S* shrub

parameter F_{LNR} to be the second most important parameter influencing model output, the most important parameter, was CN_L (Eq. 9), also a key input for the estimation of $V_{c,max}$ (Sargsyan et al. 2013). The disparity between the model representation and observation of this parameter is significant. The combination of the very low turnover rate (k_{cat}) of Rubisco and the wasteful oxygenation reaction, means that plants must make a major investment in this inefficient enzyme (Ainsworth and Rogers 2007). Values for F_{LNR} estimated from C_3 crops are c. 20 % (Evans and Seemann 1984; Mitchell et al. 2000; Leakey et al. 2009). However, the values for F_{LNR} used in ESMs are typically less than half the observed value (Fig. 2). This suggests that the lower estimates of $V_{c,max}$ (Fig. 1) for CLM and Biomes-BGC may be driven by the low values for PFT-specific F_{LNR} (Fig. 2). For some PFTs the estimate used for F_{LNR} is arbitrary (Biome-BGC, CLM). Clearly, more data are required to improve confidence in proscribed F_{LNR} values. Calculation of F_{LNR} also revealed that the value used by BETHY to represent C_3 crops closely matches the widely reported value of c. 20 % (Fig. 3). This suggests that application of PFT-specific values of F_{LNR} derived from BETHY in models that estimate $V_{c,max}$ mechanistically from N_a (Biome-BGC, CLM) would markedly increase $V_{c,max}$ in these models, and may offer a better source of parameterization than current sources.

Biome-BGC, CLM, Hybrid, and JULES currently assume that the amount of *N* invested in Rubisco does not change with N_a and fix that parameter for each PFT, either directly or through PFT-specific N_a and SLA values. However, there is considerable evidence that this is not the case when variation in F_{LNR} with N_a is examined in a single species (Wong 1979; Evans 1989; Makino et al.

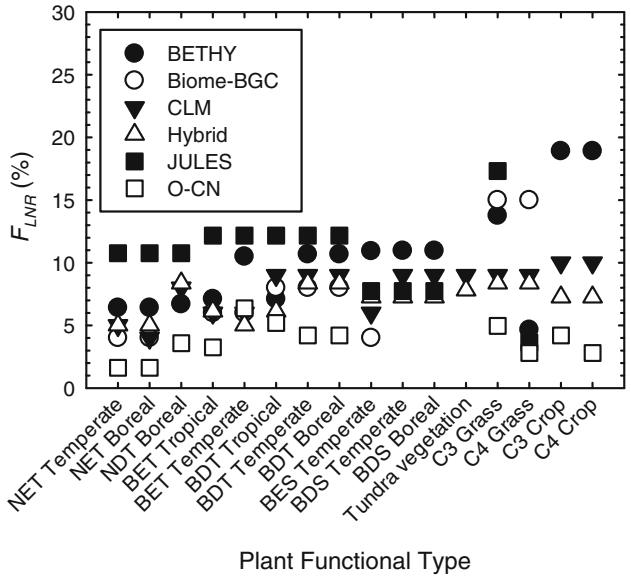

Fig. 2 The fraction of leaf *N* invested in Rubisco (F_{LNR}, %) for 16 Plant Functional Types (PFTs). F_{LNR} was either provided in the model description (Biome-BGC, CLM) or was calculated from $V_{c,max}$ and N_a following Eq. 8 and 13 assuming, $F_{NR\%} = 16.07$ and $\alpha_{R25} = 47.34$ μmol CO_2 g^{-1} Rubiscio s^{-1}. For a given PFT a value for F_{LNR} was assigned from each model based on the similarity to the original PFT description. Where a PFT is delineated to a greater extent than in the original model the most appropriate F_{LNR} value is repeated for that PFT division. Where no F_{LNR} value was assigned to a PFT, no data was included from that model. BETHY classified tropical trees based on soil type (Table 1). The mean of the F_{LNR} for oxisols and non-oxisols calculated for BETHY was used to represent both tropical PFTs in this figure. PFT abbreviations; *N* needle leaf, *B* broad leaf, *E* evergreen, *D* deciduous, *T* tree, *S* shrub

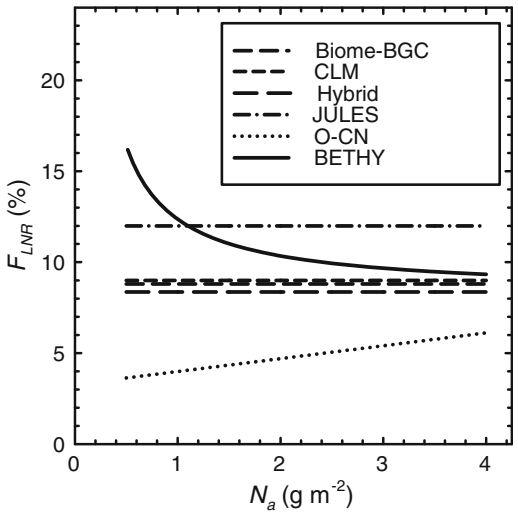

Fig. 3 The fraction of leaf *N* invested in Rubisco (F_{LNR}, %) as a function of leaf *N* content (N_a, g m^{-2}) for the Plant Functional Type–Temperate broad leaf deciduous trees. It was possible to calculate the response of F_{LNR} to N_a for six models based on $V_{c,max}$ and N_a following Eq. 8 and 13 assuming, $F_{NR\%} = 16.07$ and $\alpha_{R25} = 47.34$ μmol CO_2 g^{-1} Rubisco s^{-1}. Biome-BGC and CLM had fixed proscribed parameters for F_{LNR}, Hybrid and JULES did not proscribe F_{LNR} but F_{LNR} did not vary with N_a

1992; Theobald et al. 1998). For example, Evans (1989) showed that in spinach the investment in Rubisco increased from 10 to 19 % as N_a increased from 1.05 to 2.80 g m^{-2}. The response of F_{LNR} to N_a in temperate broad leaf deciduous trees is shown for the models where it was possible to calculate this response (Fig. 3). O–CN uses the work of Evans (1989) to adjust F_{LNR} as a function of N_a (Eq. 3 and 4). Because the linear relationships used in BETHY (Ziehn et al. 2011) have positive i_v values (Eq. 1) BETHY decreases F_{LNR} as N_a rises (Fig. 3). Experiments designed to elucidate PFT-specific relationships between F_{LNR} and N_a would provide valuable data for estimating $V_{c,max}$, particularly at low N_a, where the estimation of $V_{c,max}$ from N_a is markedly impacted by the intercept of these relationships. One approach used to determine F_{LNR} requires estimates of $V_{c,max}$ from leaf level gas exchange and determination of N_a in the same tissue. Fixed parameters are then used to calculate F_{LNR} (Eq. 8) as described previously (Leakey et al. 2009). Alternatively, Rubisco can be extracted from leaf tissue and the activity or amount determined biochemically and compared with total leaf protein (Evans 1989; Makino et al. 1992).

The fraction of N in the Rubisco holoenzyme (F_{NR})

The parameter F_{NR} is more commonly expressed as the percentage of *N* in the Rubisco molecule relative to the total molecular mass of the holoenzyme, termed $F_{NR\%}$ here. In CLM and Biome-BGC, $F_{NR\%}$ is 13.96 % (Kuehn and McFadden 1969; Thornton and Zimmermann 2007).

$$F_{NR\%} = \frac{100}{F_{NR}} \tag{13}$$

Given that Rubisco is highly conserved, there is a surprising range (13.96–16.36 %) of reported values for $F_{NR\%}$ (Steer et al. 1968; Evans and Seemann 1984; Niinemets and Tenhunen 1997; Thornton and Zimmermann 2007). Estimation of $F_{NR\%}$ is possible based on the amino acid composition of form I (L_8S_8) of the mature holoenzyme and well-documented post translational modification that includes methylation and *N* terminal processing (Spreitzer and Salvucci 2002; Houtz and Portis 2003). The amino acid sequences of the large (accession NP_054944.1, NCBI) and small (P00870, UniProtKB/Swiss-Prot) subunits of *Spinacia oleracea* (Martin 1979; Schmitz-Linneweber et al. 2001) were used here to calculate an $F_{NR\%}$ of 16.07 %. Substituting 16.07 for 13.96 in Eq. 8 and 10, would decrease the estimated $V_{c,max}$ in CLM and Biome-BGC by c. 13 %. It is possible that the difference between the estimate provided here, and that used in CLM and Biome-BGC, is due to subtraction of the mass associated with the formation of peptide bonds which appears to have been omitted in the CLM and Biome-BGC estimate.

Specific activity

Although CLM (α_{R25}) and Biome-BGC (*ACT*) use a fixed value for specific activity, it can be calculated from the k_{cat}, the number of available active sites in Rubico (S_R), and the molecular mass of the holoenzyme (M_R, g mol^{-1}), implicit is the assumption that Rubisco is fully activated, i.e., $S_R = 8$ active sites, but see below.

$$\alpha_{R25} = \frac{k_{cat} \times S_R}{M_R} \quad (14)$$

The specific activity cited in CLM and Biome-BGC is 60 μmol CO_2 g^{-1} Rubisco s^{-1}. The molecular mass and activation state of Rubisco are not quoted in the technical descriptions (Biome-BGC 2010; Oleson et al. 2010), the supporting reference (Thornton and Zimmermann 2007) or the available proximal reference (Woodrow and Berry 1988). However, the k_{cat} is listed as 3.3 s^{-1} site^{-1} (Woodrow and Berry 1988). Based on this k_{cat}, and the assumption that the specific activity was estimated with a saturating CO_2 concentration, a fully activated Rubisco with a molecular mass of 575 kDa (see below) would result in a specific activity of only 46 μmol CO_2 g^{-1} Rubisco s^{-1}. Holding all other variables constant, and assuming full activation of Rubisco, substituting this value into Eq. 8 and 10 would result in an estimate of $V_{c,max}$ that is 23 % lower than the value used by CLM and Biome-BGC.

Molecular mass of the Rubisco holoenzyme (M_R)

There is considerable variation in the molecular mass of the holoenzyme that results from variation in reported values for both the large subunit (Lsu) and small subunit (Ssu) of Rubisco (Andersson and Backlund 2008). The mass of the Lsu (56,629 Da) and Ssu (15,193 Da) calculated from the *Spinacia oleracea* amino acid sequence (above) results in a holoenzyme that is 574,575 Da, which is just under 3 % higher than the commonly cited 560 kDa estimate for land plants and green algae (Spreitzer and Salvucci 2002). The mass estimated from the sequence is probably within the margin of error (6 or 7 residues per subunit) when estimating the molecular mass of the Lsu and Ssu using SDS-PAGE approaches. Equations 8 and 14 show that the small (less than 3 %) impact of changes in M_R is inversely proportion to the projected $V_{c,max}$.

k_{cat}

The k_{cat} of Rubisco from higher plants has been reported to range from 2.5 to 5.4 s^{-1} (Tcherkez et al. 2006). Values differ between species, habitats, techniques, and laboratories (Makino et al. 1988; von Caemmerer et al. 1994; Sage 2002; Tcherkez et al. 2006; Kubien et al. 2008; Cousins et al. 2010). In the absence of robust PFT-specific parameterization of k_{cat}, ESMs need a well-constrained estimate for broad application. Recent in vitro measurements have begun to converge (Kubien et al. 2008; Whitney et al. 2009; Cousins et al. 2010) and closely match earlier estimates made in vivo using antisense-Ssu transgenic tobacco (von Caemmerer et al. 1994). While PFT-specific k_{cat} values are not yet available, it is clear that C_3 and C_4 specific values for k_{cat} should be considered for implementation in ESMs, although uncertainty surrounding the C_4 k_{cat} values is greater than k_{cat} estimates for C_3 species (Sage 2002; Kubien and Sage 2004; Kubien et al. 2008). Current recommended values for the k_{cat} in C_3 and C_4 species are 3.4 and 4.4 s^{-1}, respectively (von Caemmerer et al. 1994; Kubien et al. 2008; Whitney et al. 2009; Cousins et al. 2010). Estimation of PFT-specific k_{cat}, and other kinetic constants, is a much needed area of active research, and attention should be paid to this emerging literature. Equations 8 and 14 show that changes in k_{cat} are directly proportional to estimation of $V_{c,max}$. Unlike purely empirical models, the approach taken by CLM and Biome-BGC allows new PFT-specific data on enzyme kinetics to be readily incorporated into the models as it becomes available.

Activation (S_R)

Rubisco must be activated through reversible carbamylation of a lysine residue and binding of Mg^{2+}. Rubisco is usually fully active and carbamylated at current [CO_2], steady-state saturating light, and optimum temperatures (von Caemmerer and Quick 2000; Portis 2003). Current ESMs assume constant and high activation states. However, for many PFTs, especially those with a high leaf area index in biomes where rising temperatures will push operating temperatures above thermal optima, this assumption may not be valid. The activation state of Rubisco is not incorporated into current ESMs, but could be, as described previously (Sage et al. 2008). PFT-specific estimates of activation for a given set of environmental conditions can be readily determined following rapid extraction of the enzyme and comparison of initial and fully activated enzyme activity (Rogers et al. 2001). Activation is important to represent in models where $V_{c,max}$ is mechanistically linked to N acquisition because the impact on N availability could be significant. For example, if Rubisco was 80 % activated, it would require a 25 % increase in N_a to match the $V_{c,max}$ obtained if Rubisco were fully activated (Eq. 8 and 14).

Model calibration

Model calibration, or to use the more provocative term, tuning, is an approach that modeling groups use to match

model outputs with site-specific or remotely sensed measurements of NPP or GPP (AVIM, CTEM). This makes sense because the models need to be able to reproduce current C stocks and fluxes if we are to have any confidence in their ability to project future responses. $V_{c,max}$ is an excellent parameter to use for tuning because the impact on GPP and NPP is direct and tightly coupled to model output (Sargsyan et al. 2013). Therefore, relatively simple tuning of $V_{c,max}$ to match observed NPP or GPP can be used to compensate for deficiencies in other areas of the model (Bonan et al. 2011). Some models set $V_{c,max}$ directly through tuning exercises (AVIM, CTEM) and others adjust best estimates of $V_{c,max}$ through subsequent tuning of $V_{c,max}$ (CTEM 1.1) or the coefficients used to adjust it (Hybrid, n_2; JULES, n_l). A major problem of tuning the models using $V_{c,max}$ is that the response of photosynthesis to rising CO_2 concentration is determined largely by the investment plants make in Rubisco. Plants with a larger investment in Rubisco, and a large $V_{c,max}$, typically have a higher photosynthetic rate but are less responsive to rising CO_2 concentration because photosynthesis becomes limited by the capacity to regenerate ribulose-1,5-bisphophate at a lower [CO_2] than plants with a smaller $V_{c,max}$. This is why trees typically show a greater percent stimulation in photosynthesis at elevated [CO_2] when compared with C_3 crops (Ainsworth and Rogers 2007). Since a principal goal of ESMs is the projection of future [CO_2], tuning models with a parameter that directly impacts the CO_2 responsiveness of the future terrestrial biosphere needs careful consideration. Of course, it is possible that current plant trait data and model representation of plant physiology are not sufficient to provide accurate model outputs without tuning.

Conclusion

The ESMs surveyed in this study seek to represent the CO_2 uptake of the same biomes using similarly, and in some cases identically, defined PFTs, yet the variation in the $V_{c,max}$ between the different models is substantial. This is unacceptable in the given currently available resources and the critical role that $V_{c,max}$ plays in determining global C flux. ESMs need to take greater advantage of plant trait data bases, e.g., TRY (Kattge et al. 2011) to constrain the PFT-specific estimates used for key parameters such as SLA, CN_L, N_a, C_m, F_{LNR}, where relevant $V_{c,max}$ directly, and to do that using parameterization approaches that minimize the uncertainty in model outputs (Kattge et al. 2009; Ziehn et al. 2011; Alton 2011; Wang et al. 2012). We also need to continue to expand plant trait databases to reduce uncertainty in existing PFT parameterization, which can be large. This is particularly important for PFTs in under-represented biomes, biomes that dominate global C fluxes, or those that are particularly vulnerable to global change, such as PFTs in Arctic and Tropical ecosystems. In addition to identifying the approaches used to estimate $V_{c,max}$, and the wide range of resulting values, this study also identified some alternatives to the fixed parameters used by CLM and Biome-BGC. If the suggested changes in k_{cat}, F_{NR} and M_R were implemented, it would collectively reduce estimated $V_{c,max}$ in these models by 31 % for C_3 species and 11 % for C_4 species. These reductions in $V_{c,max}$ may be offset if potential increases in PFT specific F_{LNR} are also implemented.

The range of PFTs and their physiological characterization should also be expanded to enable more accurate and dynamic representation of plant communities and their response to global change. In particular, variation in $V_{c,max}$ due to long-term acclimation to growth at rising temperature and [CO_2] is currently absent from most ESMs (Smith and Dukes 2012). Because the movement of CO_2 from the atmosphere to the chloroplast plays a major role in determining CO_2 responsiveness, it also will be critical to improve understanding and model representation of the limitation on photosynthesis imposed by stomatal and mesophyll conductance. In short, as increasing computing power allows it, we need to expand the representation of plant physiology in ESMs.

Acknowledgments The Author is grateful to Vivek Arora, Douglas Clark, Rosie Fischer, Jinjun Ji, David Kubien, Joe Melton, Jared Oyler, Steve Running, Khachik Sargsyan, Peter Thornton, and Weile Wang for sharing unpublished work, providing model parameters and useful discussion. The author is also grateful for the constructive criticism received from two anonymous reviewers. This study was supported by Laboratory Directed Research and Development funds at Brookhaven National Laboratory, by The Next-Generation Ecosystem Experiments (NGEE Arctic) project that is supported by the Office of Biological and Environmental Research in the Department of Energy, Office of Science, and through the United States Department of Energy contract No. DE-AC02-98CH10886 to Brookhaven National Laboratory.

References

Ainsworth EA, Rogers A (2007) The response of photosynthesis and stomatal conductance to rising CO_2: mechanisms and environmental interactions. Plant, Cell Environ 30:258–270

Alton PB (2011) How useful are plant functional types in global simulations of the carbon, water, and energy cycles? J Geophys Res Biogeosci 116:G01030

Andersson I, Backlund A (2008) Structure and function of rubisco. Plant Physiol Biochem 46:275–291

Arora VK (2003) Simulating energy and carbon fluxes over winter wheat using coupled land surface and terrestrial ecosystem models. Agric For Meteorol 118:21–47

Arora VK, Boer GJ (2010) Uncertainties in the 20th century carbon budget associated with land use change. Glob Chang Biol 16:3327–3348

Arora VK, Boer GJ, Friedlingstein P, Eby M, Jones CD, Christian JR, Bonan G, Bopp L, Brovkin V, Cadule P, Hajima T, Ilyina T, Lindsay K, Tjiputra JF, Wu T (2013) Carbon-concentration and carbon-climate feedbacks in CMIP5 Earth system models. J Clim. doi:10.1175/JCLI-D-12-00494.1

Bauerle WL, Oren R, Way DA, Qian SS, Stoy PC, Thornton PE, Bowden JD, Hoffman FM, Reynolds RF (2012) Photoperiodic regulation of the seasonal pattern of photosynthetic capacity and the implications for carbon cycling. Proc Natl Acad Sci USA 109:8612–8617

Beer C, Reichstein M, Tomelleri E, Ciais P, Jung M, Carvalhais N, Rodenbeck C, Arain MA, Baldocchi D, Bonan GB, Bondeau A, Cescatti A, Lasslop G, Lindroth A, Lomas M, Luyssaert S, Margolis H, Oleson KW, Roupsard O, Veenendaal E, Viovy N, Williams C, Woodward FI, Papale D (2010) Terrestrial gross carbon dioxide uptake: global distribution and covariation with climate. Science 329:834–838

Berbigier P, Bonnefond JM, Mellmann P (2001) CO_2 and water vapour fluxes for 2 years above euroflux forest site. Agric For Meteorol 108:183–197

Bernacchi CJ, Singsaas EL, Pimentel C, Portis AR, Long SP (2001) Improved temperature response functions for models of rubisco-limited photosynthesis. Plant, Cell Environ 24:253–259

Biome-BGC (2010) Biome BGC version 4.2: Thoeretical framework of BIOME-BGC. http://www.ntsg.umt.edu/project/biome-bgc. Available at 3 April 2013

Boden TA, Marland G, Andres RJ (2012) Global, regional and national fossil-fuel CO_2 emissions. Carbon Dioxide Information Analysis Center, Oak Ridge National Laboratory, U.S. Department of Energy, Oak Ridge

Bonan GB (1996) A land surface model (LSM version 1.0) for ecological, hydrological, and atmospheric studies: Technical description and user's guide. National Center for Atmospheric Research, Boulder

Bonan GB, Lawrence PJ, Oleson KW, Levis S, Jung M, Reichstein M, Lawrence DM, Swenson SC (2011) Improving canopy processes in the community land model version 4 (CLM4) using global flux fields empirically inferred from fluxnet data. J Geophys Res Biogeosci 116:G02014

Bonan GB, Oleson KW, Fisher RA, Lasslop G, Reichstein M (2012) Reconciling leaf physiological traits and canopy flux data: use of the try and fluxnet databases in the community land model version 4. J Geophys Res Biogeosci 117:G02026

Canadell JG, Le Quere C, Raupach MR, Field CB, Buitenhuis ET, Ciais P, Conway TJ, Gillett NP, Houghton RA, Marland G (2007) Contributions to accelerating atmospheric CO_2 growth from economic activity, carbon intensity, and efficiency of natural sinks. Proc Natl Acad Sci USA 104(47):18866–18870

Clark DB, Mercado LM, Sitch S, Jones CD, Gedney N, Best MJ, Pryor M, Rooney GG, Essery RLH, Blyth E, Boucher O, Harding RJ, Huntingford C, Cox PM (2011) The joint UK land environment simulator (JULES), model description-part 2: carbon fluxes and vegetation dynamics. Geosci Model Dev 4(3):701–722

Cousins AB, Ghannoum O, Von Caemmerer S, Badger MR (2010) Simultaneous determination of rubisco carboxylase and oxygenase kinetic parameters in triticum aestivum and zea mays using membrane inlet mass spectrometry. Plant, Cell Environ 33:444–452

Cox PM (2001) Description of the "triffid" dynamic global vegetation model. Hadley Centre Technical Note-24

Ethier GJ, Livingston NJ (2004) On the need to incorporate sensitivity to CO_2 transfer conductance into the farquhar-von caemmerer-berry leaf photosynthesis model. Plant, Cell Environ 27:137–153

Evans JR (1989) Photosynthesis and nitrogen relationships in leaves of C-3 plants. Oecologia 78:9–19

Evans JR, Seemann JR (1984) Differences between wheat genotypes in specific activity of ribulose-1,5-bisphosphate carboxylase and the relationship to photosynthesis. Plant Physiol 74(4):759–765

Farquhar GD, von Caemmerer S, Berry JA (1980) A biochemical-model of photosynthetic CO_2 assimilation in leaves of C-3 species. Planta 149:78–90

Foley JA, Prentice IC, Ramankutty N, Levis S, Pollard D, Sitch S, Haxeltine A (1996) An integrated biosphere model of land surface processes, terrestrial carbon balance, and vegetation dynamics. Glob Biogeochem Cycles 10:603–628

Friedlingstein P, Fung I, Holland E, John J, Brasseur G, Erickson D, Schimel D (1995) On the contribution of CO_2 fertilization to the missing biospheric sink. Glob Biogeochem Cycles 9:541–556

Friedlingstein P, Cox P, Betts R et al (2006) Climate-carbon cycle feedback analysis: results from the (cmip)-m-4 model intercomparison. J Clim 19:3337–3353

Friend AD (2010) Terrestrial plant production and climate change. J Exp Bot 61:1293–1309

Friend AD, Kiang NY (2005) Land surface model development for the giss gcm: effects of improved canopy physiology on simulated climate. J Clim 18:2883–2902

Friend AD, Stevens AK, Knox RG, Cannell MGR (1997) A process-based, terrestrial biosphere model of ecosystem dynamics (Hybrid v3.0). Ecol Model 95:249–287

Goulden ML, Munger JW, Fan SM, Daube BC, Wofsy SC (1996) Measurements of carbon sequestration by long-term eddy covariance: methods and a critical evaluation of accuracy. Glob Chang Biol 2:169–182

Gregory JM, Jones CD, Cadule P, Friedlingstein P (2009) Quantifying carbon cycle feedbacks. J Clim 22:5232–5250

Gu LH, Pallardy SG, Tu K, Law BE, Wullschleger SD (2010) Reliable estimation of biochemical parameters from C-3 leaf photosynthesis-intercellular carbon dioxide response curves. Plant, Cell Environ 33:1852–1874

Hanan NP, Burba G, Verma SB, Berry JA, Suyker A, Walter-Shea EA (2002) Inversion of net ecosystem CO_2 flux measurements for estimation of canopy par absorption. Glob Chang Biol 8:563–574

Haxeltine A, Prentice IC (1996a) Biome3: an equilibrium terrestrial biosphere model based on ecophysiological constraints, resource availability, and competition among plant functional types. Glob Biogeochem Cycles 10:693–709

Haxeltine A, Prentice IC (1996b) A general model for the light-use efficiency of primary production. Funct Ecol 10(5):551–561

Houtz RL, Portis AR (2003) The life of ribulose 1,5-bisphosphate carboxylase/oxygenase-posttranslational facts and mysteries. Arch Biochem Biophys 414(2):150–158

Ishida A, Uemura A, Koike N, Matsumoto Y, Hoe AL (1999) Interactive effects of leaf age and self-shading on leaf structure, photosynthetic capacity and chlorophyll fluorescence in the rain forest tree, dryobalanops aromatica. Tree Physiol 19:741–747

Ji JJ (1995) A climate-vegetation interaction model: simulating physical and biological processes at the surface. J Biogeogr 22:445–451

Johnson IR, Thornley JHM (1984) A model of instantaneous and daily canopy photosynthesis. J Theor Biol 107:531–545

Kattge J, Knorr W, Raddatz T, Wirth C (2009) Quantifying photosynthetic capacity and its relationship to leaf nitrogen content for global-scale terrestrial biosphere models. Glob Chang Biol 15:976–991

Kattge J, Diaz S, Lavorel S et al (2011) TRY—a global database of plant traits. Glob Chang Biol 17:2905–2935

King AW, Post WM, Wullschleger SD (1997) The potential response of terrestrial carbon storage to changes in climate and atmospheric CO_2. Clim Chang 35:199–227

Knorr W (2000) Annual and interannual CO_2 exchanges of the terrestrial biosphere: process-based simulations and uncertainties. Glob Ecol Biogeogr 9:225–252

Krinner G, Viovy N, de Noblet-Ducoudre N, Ogee J, Polcher J, Friedlingstein P, Ciais P, Sitch S, Prentice IC (2005) A dynamic global vegetation model for studies of the coupled atmosphere-biosphere system. Glob Biogeochem Cycles 19:GB1015

Kubien DS, Sage RF (2004) Low-temperature photosynthetic performance of a C_4 grass and a co-occurring C_3 grass native to high latitudes. Plant, Cell Environ 27:907–916

Kubien DS, Whitney SM, Moore PV, Jesson LK (2008) The biochemistry of rubisco in flaveria. J Exp Bot 59:1767–1777

Kucharik CJ, Foley JA, Delire C, Fisher VA, Coe MT, Lenters JD, Young-Molling C, Ramankutty N, Norman JM, Gower ST (2000) Testing the performance of a dynamic global ecosystem model: water balance, carbon balance, and vegetation structure. Glob Biogeochem Cycles 14:795–825

Kuehn GD, McFadden BA (1969) Ribulose 1,5-diphosphate carboxylase from hydrogenomonas eutropha and hydrogenomonas facilis.2. Molecular weight subunits composition and sulfhydryl groups. Biochemistry 8:2403

Kull O, Kruijt B (1998) Leaf photosynthetic light response: a mechanistic model for scaling photosynthesis to leaves and canopies. Funct Ecol 12:767–777

Kull O, Niinemets U (1998) Distribution of leaf photosynthetic properties in tree canopies: comparison of species with different shade tolerance. Funct Ecol 12(3):472–479

Leakey ADB, Ainsworth EA, Bernacchi CJ, Rogers A, Long SP, Ort DR (2009) Elevated CO_2 effects on plant carbon, nitrogen, and water relations: six important lessons from face. J Exp Bot 60:2859–2876

Levy PE, Cannell MGR, Friend AD (2004) Modelling the impact of future changes in climate, CO_2 concentration and land use on natural ecosystems and the terrestrial carbon sink. Glob Environ Chang 14(1):21–30

Long SP, Bernacchi CJ (2003) Gas exchange measurements, what can they tell us about the underlying limitations to photosynthesis? Procedures and sources of error. J Exp Bot 54:2393–2401

Lu JH, Ji JJ (2006) A simulation and mechanism analysis of long-term variations at land surface over arid/semi-arid area in north china. J Geophys Res Atmospheres 111(D9):1–22

Luyssaert S, Inglima I, Jung M et al (2007) CO_2 balance of boreal, temperate, and tropical forests derived from a global database. Glob Change Biol 13(12):2509–2537

Makino A, Mae T, Ohira K (1988) Differences between wheat and rice in the enzymic properties of ribulose-1,5-bisphosphate carboxylase oxygenase and the relationship to photosynthetic gas-exchange. Planta 174(1):30–38

Makino A, Sakashita H, Hidema J, Mae T, Ojima K, Osmond B (1992) Distinctive responses of ribulose-1,5-bisphosphate carboxylase and carbonic-anhydrase in wheat leaves to nitrogen nutrition and their possible relationships to CO_2 transfer resistance. Plant Physiol 100:1737–1743

Malhi Y, Nobre AD, Grace J, Kruijt B, Pereira MGP, Culf A, Scott S (1998) Carbon dioxide transfer over a central amazonian rain forest. J Geophys Res Atmospheres 103:31593–31612

Martin PG (1979) Amino-acid sequence of the small subunit of ribulose-1,5-bisphosphate carboxylase from spinach. Aust J Plant Physiol 6:401–408

McGuire AD, Melillo JM, Joyce LA, Kicklighter DW, Grace AL, Moore B, Vorosmarty CJ (1992) Interactions between carbon and nitrogen dynamics in estimating net primary production for potential vegetation in North America. Glob Biogeochem Cycles 6:101–124

Mitchell RAC, Theobald JC, Parry MAJ, Lawlor DW (2000) Is there scope for improving balance between rubp-regeneration and carboxylation capacities in wheat at elevated CO_2? J Exp Bot 51:391–397

Niinemets U, Tenhunen JD (1997) A model separating leaf structural and physiological effects on carbon gain along light gradients for the shade-tolerant species acer saccharum. Plant, Cell Environ 20:845–866

Oleson KW, Dai Y, Bonan GB, Bosilovich M, Dickinson R, Dirmeyer P, Hoffman FM, Houser P, Levis S, Niu G-Y, Thornton P, Vertenstein M, Yang Z-L, Zeng X (2004) Technical description of the community land model (CLM). National Center for Atmospheric Research, Boulder, Colorado

Oleson KW, Lawrence DM, Bonan GB, Flanner MG, Kluzek E, Lawrence PJ, Levis S, Swenson SC, Thornton PE (2010) Technical description of version 4.0 of the community land model (CLM). vol NCAR Technical Note. National Center for Atmospheric Research

Portis AR (2003) Rubisco activase—rubisco's catalytic chaperone. Photosynth Res 75:11–27

Potter CS, Randerson JT, Field CB, Matson PA, Vitousek PM, Mooney HA, Klooster SA (1993) Terrestrial ecosystem production—a process model-based on global satellite and surface data. Glob Biogeochem Cycles 7:811–841

Raddatz TJ, Reick CH, Knorr W, Kattge J, Roeckner E, Schnur R, Schnitzler KG, Wetzel P, Jungclaus J (2007) Will the tropical land biosphere dominate the climate-carbon cycle feedback during the twenty-first century? Clim Dyn 29:565−574

Reich PB, Walters MB, Ellsworth DS (1997) From tropics to tundra: global convergence in plant functioning. Proc Natl Acad Sci USA 94:13730–13734

Rogers A, Ellsworth DS, Humphries SW (2001) Possible explanation of the disparity between the in vitro and in vivo measurements of rubisco activity: a study in loblolly pine grown in elevated pCO_2. J Exp Bot 52:1555–1561

Sage RF (2002) Variation in the k_{cat} of rubisco in C_3 and C_4 plants and some implications for photosynthetic performance at high and low temperature. J Exp Bot 53:609–620

Sage RF, Way DA, Kubien DS (2008) Rubisco, rubisco activase, and global climate change. J Exp Bot 59:1581–1595

Sargsyan K, Safta C, Habib NN, Debusschere BJ, Ricciuto D, Thornton P (2013) Dimensionality reduction for complex models via bayesian compressive sensing. Int J Uncertain Quant (In Press)

Sato H, Itoh A, Kohyama T (2007) Seib-dgvm: a new dynamic global vegetation model using a spatially explicit individual-based approach. Ecol Model 200:279–307

Schmitz-Linneweber C, Maier RM, Alcaraz JP, Cottet A, Herrmann RG, Mache R (2001) The plastid chromosome of spinach (*Spinacia oleracea*): complete nucleotide sequence and gene organization. Plant Mol Biol 45(3):307–315

Scholze M, Kaminski T, Rayner P, Knorr W, Giering R (2007) Propagating uncertainty through prognostic carbon cycle data assimilation system simulations. J Geophys Res Atmospheres 112:D17305

Schulze ED, Kelliher FM, Korner C, Lloyd J, Leuning R (1994) Relationships among maximum stomatal conductance, ecosystem surface conductance, carbon assimilation rate, and plant nitrogen nutrition—a global ecology scaling exercise. Annu Rev Ecol Syst 25:629

Sellers PJ, Randall DA, Collatz GJ, Berry JA, Field CB, Dazlich DA, Zhang C, Collelo GD, Bounoua L (1996) A revised land surface parameterization (SIB2) for atmospheric GCMS.1. Model formulation. J Clim 9:676–705

Sitch S, Smith B, Prentice IC, Arneth A, Bondeau A, Cramer W, Kaplan JO, Levis S, Lucht W, Sykes MT, Thonicke K, Venevsky S (2003) Evaluation of ecosystem dynamics, plant geography and terrestrial carbon cycling in the LPJ dynamic global vegetation model. Glob Change Biol 9:161–185

Smith NG, Dukes JS (2012) Plant respiration and photosynthesis in global-scale models: Incorporating acclimation to temperature and CO_2. Glob Chang Biol 19:45–63

Spreitzer RJ, Salvucci ME (2002) Rubisco: structure, regulatory interactions, and possibilities for a better enzyme. Annu Rev Plant Biol 53:449–475

Steer MW, Gunning BES, Graham TA, Carr DJ (1968) Isolation properties and structure of fraction i protein from avena sativa l. Planta 79:254

Tcherkez GGB, Farquhar GD, Andrews TJ (2006) Despite slow catalysis and confused substrate specificity, all ribulose bisphosphate carboxylases may be nearly perfectly optimized. Proc Natl Acad Sci USA 103:7246–7251

Theobald JC, Mitchell RAC, Parry MAJ, Lawlor DW (1998) Estimating the excess investment in ribulose-1,5-bisphosphate carboxylase/oxygenase in leaves of spring wheat crown under elevated CO_2. Plant Physiol 118:945–955

Thornton PE, Zimmermann NE (2007) An improved canopy integration scheme for a land surface model with prognostic canopy structure. J Clim 20:3902–3923

Thornton PE, Law BE, Gholz HL, Clark KL, Falge E, Ellsworth DS, Golstein AH, Monson RK, Hollinger D, Falk M, Chen J, Sparks JP (2002) Modeling and measuring the effects of disturbance history and climate on carbon and water budgets in evergreen needle leaf forests. Agric For Meteorol 113:185–222

von Caemmerer S, Quick PW (2000) Rubisco: Physiology in vivo. In: Sharkey TD, von Caemmerer S (eds) Leegood RC. Physiology and metabolism. Kluwer Academic Publishers, Photosynthesis, pp 85–113

von Caemmerer S, Evans JR, Hudson GS, Andrews TJ (1994) The kinetics of ribulose-1,5-bisphosphate carboxylase/oxygenase in vivo inferred from measurements of photosynthesis in leaves of transgenic tobacco. Planta 195:88–97

Wang WL, Dungan J, Hashimoto H, Michaelis AR, Milesi C, Ichii K, Nemani RR (2011) Diagnosing and assessing uncertainties of terrestrial ecosystem models in a multimodel ensemble experiment: 2 Carbon balance. Glob Chang Biol 17:1367–1378

Wang YP, Lu XJ, Wright IJ, Dai YJ, Rayner PJ, Reich PB (2012) Correlations among leaf traits provide a significant constraint on the estimate of global gross primary production. Geophys Res Lett 39:L19405

White MA, Thornton PE, Running SW, Nemani RR (2000) Parameterization and sensitivity analysis of the biome-bgc terrestrial ecosystem model: net primary production controls. Earth Interact 4:1–85

Whitney SM, Kane HJ, Houtz RL, Sharwood RE (2009) Rubisco oligomers composed of linked small and large subunits assemble in tobacco plastids and have higher affinities for CO_2 and O_2. Plant Physiol 149(4):1887–1895

Wilson KB, Baldocchi DD, Hanson PJ (2000) Spatial and seasonal variability of photosynthetic parameters and their relationship to leaf nitrogen in a deciduous forest. Tree Physiol 20:565–578

Wofsy SC, Goulden ML, Munger JW, Fan SM, Bakwin PS, Daube BC, Bassow SL, Bazzaz FA (1993) Net exchange of CO_2 in a midlatitude forest. Science 260:1314–1317

Wong SC (1979) Elevated atmospheric partial-pressure of CO_2 and plant-growth 1. Interactions of nitrogen nutrition and photosynthetic capacity in C3 and C4 plants. Oecologia 44:68–74

Woodrow IE, Berry JA (1988) Enzymatic regulation of photosynthetic CO_2 fixation in C-3 plants. Ann Rev Plant Physiol Plant Mol Biol 39:533–594

Woodward FI, Lomas MR (2004) Vegetation dynamics—simulating responses to climatic change. Biol Rev 79:643–670

Wullschleger SD (1993) Biochemical limitations to carbon assimilation in C_3 plants—a retrospective analysis of the a/ci curves from 109 species. J Exp Bot 44:907–920

Xu LK, Baldocchi DD (2003) Seasonal trends in photosynthetic parameters and stomatal conductance of blue oak (*Quercus douglasii*) under prolonged summer drought and high temperature. Tree Physiol 23:865–877

Xu R, Prentice IC (2008) Terrestrial nitrogen cycle simulation with a dynamic global vegetation model. Glob Chang Biol 14:1745–1764

Zaehle S, Friend AD (2010) Carbon and nitrogen cycle dynamics in the O–CN land surface model: 1. Model description, site-scale evaluation, and sensitivity to parameter estimates. Glob Biogeochem Cycles 24:GB1005

Zeng N, Qian HF, Munoz E, Iacono R (2004) How strong is carbon cycle-climate feedback under global warming? Geophys Res Lett 31:202–203

Zhang YJ, Xu M, Chen H, Adams J (2009) Global pattern of npp to gpp ratio derived from modis data: effects of ecosystem type, geographical location and climate. Glob Ecol Biogeogr 18:280–290

Ziehn T, Kattge J, Knorr W, Scholze M (2011) Improving the predictability of global CO_2 assimilation rates under climate change. Geophys Res Lett 38:1513–1531